

OPEN ACCESS

EDITED BY
Jinyang Wu,
Shanghai Jiao Tong University, China

REVIEWED BY Hongyang Ma, Peking University Hospital of Stomatology, China Chuxi Zhang,

*CORRESPONDENCE
Fritzie I. Arce-McShane
☑ fritziea@uw.edu

Fudan University, China

RECEIVED 26 June 2025 ACCEPTED 27 August 2025 PUBLISHED 17 September 2025

CITATION

Li JS, Ramsay DS, Burke AB, Huang GJ and Arce-McShane FI (2025) An integrated approach to tracking mandibular position relative to incisal and condylar envelopes of motion during intraoral clinical procedures: a new look at TMJ movements.

Front. Dent. Med. 6:1654118.

doi: 10.3389/fdmed.2025.1654118

COPYRIGHT

© 2025 Li, Ramsay, Burke, Huang and Arce-McShane. This is an open-access article distributed under the terms of the Creative Commons Attribution License (CC BY). The use, distribution or reproduction in other forums is permitted, provided the original author(s) and the copyright owner(s) are credited and that the original publication in this journal is cited, in accordance with accepted academic practice. No use, distribution or reproduction is permitted which does not comply with these terms.

An integrated approach to tracking mandibular position relative to incisal and condylar envelopes of motion during intraoral clinical procedures: a new look at TMJ movements

Jing-Sheng Li¹, Douglas S. Ramsay^{1,2}, Andrea B. Burke³, Greg J. Huang² and Fritzie I. Arce-McShane^{1*}

¹Department of Oral Health Sciences, University of Washington School of Dentistry, Seattle, WA, United States, ²Department of Orthodontics, University of Washington School of Dentistry, Seattle, WA, United States, ³Department of Oral and Maxillofacial Surgery, University of Washington School of Dentistry, Seattle, WA, United States

Current methods for tracking temporomandibular joint (TMJ) movements are difficult to perform during dental procedures. Yet precise and accurate quantification of mandibular movements is critical for understanding temporomandibular biomechanics and how certain movements may contribute to temporomandibular dysfunction. This is particularly relevant to clinical procedures that might move the mandible near or beyond its functional range of motion. We present a novel approach that integrates cone-beam computed tomography, optical intra-oral scans, and six degreeof-freedom electromagnetic sensor data to quantify mandibular movements. This method employs rigid body transformations to generate subject-specific three-dimensional (3D) envelopes of motion and assess whether incisal and condylar landmarks remain within their functional 3D envelopes of motion. We demonstrate the clinical utility of this approach through simulated mandibular poses presented relative to the limits of incisal and condylar envelopes created from that individual's voluntary border movements. Our findings reveal that condylar or incisal points in simulated mandibular poses are located beyond their normal motion envelopes, highlighting the importance of simultaneous monitoring of incisal and condylar landmarks. This methodology provides a clinically relevant tool for understanding temporomandibular biomechanics and it has the potential to signal clinicians when jaw movements during dental and oral surgical procedures approach or exceed the jaw's functional range of motion and such corrective feedback could prevent adverse effects on the TMJ.

KEYWORDS

TMJ, TMD, kinematics, envelope of motion, imaging, oral surgery, dental procedure

Introduction

Temporomandibular disorder (TMD) is the second most common chronic musculoskeletal condition after chronic low back pain, affecting 5%–12% of the population at a cost of approximately \$4 billion annually (1, 2). TMD is an umbrella term that encompasses numerous clinical conditions involving the masticatory muscles, the temporomandibular joint (TMJ), and associated nerves and tissues (2). With more than 30 TMDs in the expanded taxonomy (2), research investigating the diagnosis, etiology, prevention, and optimal treatment of TMDs is critical.

Injury serves as a triggering factor for TMDs (3-8) as evidenced by a prospective study (5) that revealed a 4-fold elevated risk of TMD onset following jaw injury. Ohrbach and Sharma (7) recently concluded that "Injury can qualify as a true etiology for TMDs". The unexpected nature of injuries hinders a detailed clinical investigation of the mandibular movements during injury that are associated soft structures being stretched, compressed, or damaged. However, elective intraoral clinical procedures, such as third molar removal (3MR), would be amenable to detailed kinematic investigation. A systematic review (9) of 3MR and the subsequent development of signs and symptoms of TMD concluded that they are associated and influenced by factors such as: gender, age, third molar location, severity of impaction, and surgical difficulty. To explain this association, Huang and colleagues (4, 10) hypothesized that during 3MR, the mandible is positioned in ways that could potentially harm the TMJ complex. These injuries may subsequently contribute to the development of orofacial pain/TMD symptoms. Testing this hypothesis requires measuring mandibular movements relative to cranial structures intraoperatively during 3MR. Currently available mandibular tracking methods are not suitable for use during surgery other than surgical navigation system (e.g., large appliances placed intraorally, optical line of sight required throughout surgery, magnetic field source placement that interferes with surgical access) (11). The goals of this project were to develop a method that could be used intraoperatively and to demonstrate its application.

The TMJ functions as a bilateral synovial joint, located where the mandible's right and left condyles articulate with the articular fossa and articular eminence of the temporal bone. A fibrocartilaginous articular disc is positioned between the poorly congruent articulating surfaces of the condyle and the temporal bone. Discal ligaments attach the condyle to the disc, which allow the disc to move along with the condyle as it translates (glides) along the articular eminence while also limiting the condyle to rotational movements in the lower joint compartment (12). Other ligaments are pertinent to TMJ function (12-14). For example, the bilateral temporomandibular ligament (TML), which connects from the articular eminence at the articular tubercle to the condylar neck reinforces the lateral aspect of the capsule. The TML and capsule limit the condyle from being distracted from the articular eminence, and the TML would tense on retrusion, especially the one-sided retrusion that occurs with ipsilateral excursion. The stylomandibular ligament, which connects from styloid process of the temporal bone to the angle of the mandible, has been suggested to protect the TMJ by limiting mandibular protrusion (15). The sphenomandibular ligament connects from the sphenoid spine to the lingula of the mandible and is not thought to play a significant role in mandibular movement, although it has been suggested to limit excessive translation of the condyle after 10° of opening (15).

The anatomical interplay between the mandibular fossa of the temporal bone and mandibular condyles, together with other tissues surrounding the TMJ, are crucial for a comprehensive understanding of TMJ biomechanics. The mandible can move in 6 degrees of freedom (dof) because the condyle and the temporal bone are regarded for kinematic purposes as separate rigid bodies in space. Although the mandible can move with 6dof, its position does have some constraints from surrounding structures, such as articular surfaces of the temporal bone, occlusion of upper and lower teeth, muscles, and ligaments. The mandible makes 2,000 or more movements per day (16). Mandibular movements are commonly portrayed using an incisal envelope of movements, or Posselt's envelope (17-19), that is generated using paths traced by a reproducible landmark often on a mandibular central incisor (e.g., medial incisal corner). The vast majority of movements fall within the envelope of border movements (20, 21) such as those that occur during speaking, biting, chewing, and swallowing. The more extreme border movements of the mandible are thought to be constrained by anatomic limitations of the masticatory system that include skeletal, dental, ligamentous and muscular components as well as by proprioceptive and pain perception (22).

Various tracking systems have been developed to study the kinematics of the mandible, such as mechanical-linkage (23), optoelectronic (24–26), electromagnetic (21, 27), radiographic (28, 29), or ultrasonic systems (23). Early mechanical methods like pantographs and axiography provided limited spatial resolution. Radiographic methods offer detailed spatial resolution but expose patients to ionizing radiation. Ultrasonic systems are non-invasive and affordable but suffer from lower accuracy and are susceptible to ambient noise and reflections. A recent review (11) comparing these systems reports that ultrasonic tracking and axiography are fast and cost-effective but have higher measurement errors compared to optoelectronic and electromagnetic systems.

Incisal point-based kinematics has been widely used clinically due to the ease of tracking an incisal point and the simplicity of describing its kinematics, and it may provide clinical insights into normal and pathological conditions as they reflect the neuromuscular control of the mandibular motion (20, 21). However, tracking a single point to illustrate mandibular motion is problematic because it cannot describe the movements being made by the mandible given that a point can move with 3dof while the mandible can move with 6dof (30-32). With the use of subject-specific morphology from medical imaging, such as computed tomography (CT), cone-beam computed tomography (CBCT), or magnetic resonance imaging (MRI), current optoelectronic and electromagnetic methods could describe the condylar movements (25, 27, 33, 34) but have not been used extensively to track TMJ movements during dental procedures. The optoelectronic tracking system often mounts markers from

the extension of the teeth that may directly interfere with performing intraoral clinical procedures. Also, it requires line-of-sight and can interfere with dental procedures or require clinicians to change their preferred posture due to cameras and markers that obstruct the operating field. In contrast, electromagnetic tracking systems (21, 27, 33, 35) do not require line-of-sight, supporting its potential use during dental procedures.

Here, we present a workflow of tracking subject-specific mandibular movements during intraoral clinical procedures. The proposed method uses CBCT, optical intra-oral scans, electromagnetic 6dof sensors, and a small magnetic field source, to estimate 3D mandibular positions and orientations relative to the cranium. Also, we present case simulations of bilateral condylar position and orientation near or beyond an individual's envelopes of motion. This approach will allow clinicians to gain a better understanding of the mandibular functional dynamics during treatment, and lead to better-informed decisions about the prevention, diagnosis, and treatment of TMD and other TMJ-related pathologies.

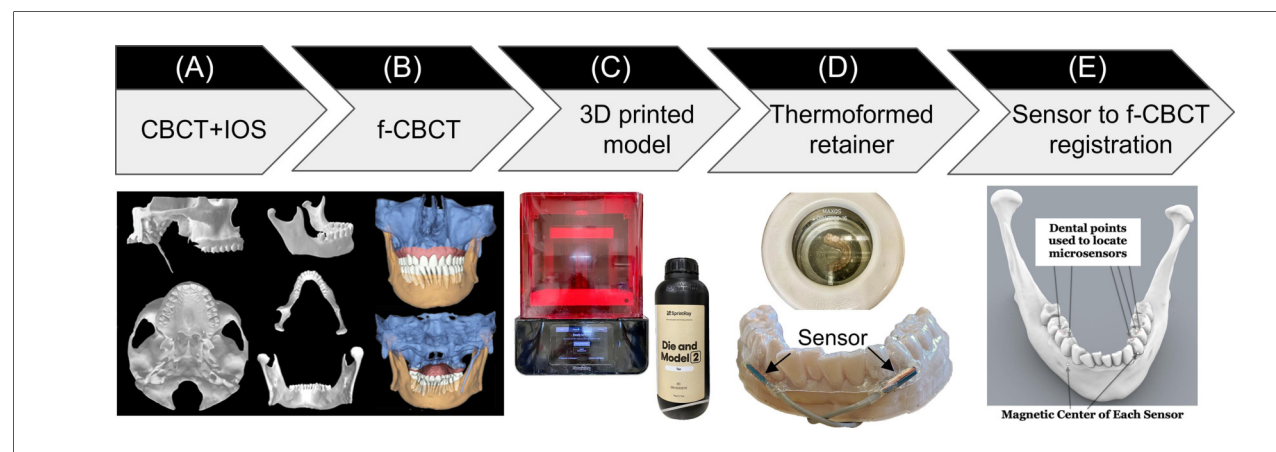
Methods

The workflow starts from the creation of a custom retainer to house the microsensors for the mandible, followed by a case study to demonstrate how to collect a range of mandibular movements for generating incisal and condylar envelopes of movement during dynamic voluntary jaw movements. Four simulated poses demonstrate the interaction between the simulated incisal and condylar points.

Creation of sensor-embedded retainer

This manufacturing process started with creating a fused conebeam computed tomography (f-CBCT) to construct a precise 3D morphology of the patient's dentition and craniofacial structures. A CBCT scan (3D Accuitomo 170, J. Morita, Saitama, Japan) is fused with an intra-oral scan (IOS, iTero Element Plus Imaging System, Align Technology, Tempe, Arizona, USA), to create a f-CBCT that provides a morphological description in submillimeter scale (Figure 1A). The CBCT scan was taken with the upper and lower teeth together at the Maximal Intercuspation (MIP) position using a field of view of 140 × 100 mm with a voxel size of 0.270 mm. The CBCT images included the cranial and maxillary complex, TMJ, and mandible. Using parallel confocal imaging technology with optical and laser scanning, the IOS captured the high-accuracy surface geometry and color of the maxillary and mandibular teeth and soft tissues. The CBCT and the IOS images were uploaded to Relu (Leuven, Belgium). Relu automatically segmented the mandible from the craniomaxillary complex and individually segmented teeth from the IOS that were then superimposed on CBCT crowns to create an optimized hybrid image of optically scanned tooth crowns and gingiva from the IOS onto the CBCT to create a fused-CBCT (f-CBCT) (Figure 1B). The gingiva on the mandible in the f-CBCT was omitted in our current application. The fusion is performed by Relu's proprietary AI algorithm that demonstrates time-efficiency and sub-voxel accuracy (36). This step is very important because the high-resolution IOS image on the f-CBCT allows us to identify idiosyncratic dental features that are also visible on the patient's mandibular model.

Maxillary and mandibular models were 3D printed (SprintRay, Los Angeles, CA) from the IOS scans. This 3D-printed mandibular model was used to fabricate the sensor-embedded retainer, designed to be comfortable and minimally thick to allow the participant to put the teeth together as close to MIP as possible. Two "dummy" six-degrees-of-freedom (6dof) micro electromagnetic sensors (Micro Sensor 1.8, Polhemus, Colchester, VT) were placed buccal to the mandibular crowns of the canine and first premolar near the gingival margin on the right and left sides (Figure 1C). The retainer has strong retention, being created using biocompatible thermoforming material (Zendura FLX, 0.76 mm thick, Bay



Sensor-embedded retainer for kinematic tracking. (A) Cone-beam computed tomography (CBCT) and intraoral scans (IOS). (B) CBCT and IOS were registered to create high-resolution fused-CBCT (f-CBCT). (C) 3D printed f-CBCT model as a mold for retainer creation. (D) Use dental vacuum forming machine to make sensorembedded retainer. (E) Use dental points to locate microsensors in 3D space.

Materials, Fremont, CA) with the heat pressure-form machine and can be easily trimmed to fit over the crowns of the upper and lower teeth. The dummy sensors were removed from the lower retainer and the actual sensors were inserted in their places. After the lower model had been coated with silicone separating medium to prevent adhesion, light cure aligner adhesive (Bond Aligner, Reliance Orthodontic Products, Itasca, IL) was applied around each microsensor in the retainer. The retainer was then fitted on the lower model's teeth, and the adhesive was light-cured to fix the microsensors in the retainer (Figure 1D). Precise 1-mm holes were placed through the retainer centered over each unique dental feature previously identified as visible on both models and on the f-CBCT. To determine the position of two microsensors with respect to the f-CBCT (Figure 1E), the subject wore the lower retainer and the tip of a hand-held 6dof stylus (3D Digitizer, Polhemus, Colchester, VT) was inserted into each hole in the retainer to touch the dental feature. The digitizing stylus located each previously defined dental features relative to the simultaneously located microsensors which were then registered through an interactive closest point method (37) on the f-CBCT. This allows 3D animation of mandibular movements tracked by the microsensors.

Mandibular motion capture

A co-author participated as a subject (a healthy male, age 66, with no history of TMD symptoms related to jaw movements). We followed the workflow above to create a custom sensor-embedded retainer. Four 6dof sensors (RX2 Standard Sensor, Polhemus, Colchester, VT) were placed on the forehead to serve as reference points for jaw movements and the retainer with two microsensors was placed on the mandibular teeth. While wearing the sensor-embedded mandibular retainer, the participant was instructed to perform a series of jaw movements in the sagittal, coronal, and transverse planes (38). After a warm-up session, we recorded a dataset comprised of 5 repetitions of each of the following movement tasks: 1) Mouth opening from MIP position and closing, 2) Jaw moving laterally to the far right or left from MIP position, 3) Jaw moving forward or backward from MIP position, 4) combined movements: mouth opening at ~6 mm, 25%, 50%, 75% and 100% from MIP position, and then jaw moving laterally to far right or left, or starting at maximum protruded position, and jaw moving laterally to far right or left (Figure 2). To reduce intra-subject variability, the participant was instructed to practice these jaw movements days prior to the data collection. Maximum values of jaw movements were determined by the most extreme value of the five repetitions of the movement.

The sampling rate for these recordings was set at 240 Hz to ensure high-resolution data capture. No additional hardware filtering was applied during data collection. According to the data sheet from the manufacturer, the electromagnetic tracking system has a spatial resolution of 0.0010 mm in 30 cm range and 0.0003 degree orientation with a static accuracy or 0.38 mm RMS for X, Y, or Z receiver position, and 0.10 degree RMS for receiver orientation (39).

Postprocessing

The first step is to orient the f-CBCT in a common frame and interpretable coordinate system. We describe the movement using the cranial coordinate system based on the maxillary occlusal plane, and anatomical alignments (40). The XYZ axes correspond to movements along the medial-lateral (left-right), anterior-posterior (front-back), and superior-inferior (up-down) directions, respectively. The X-axis represents the anteroposterior direction, the Y-axis represents the transverse (buccolingual) direction, and the Z-axis represents the vertical direction. Specific definitions are in the Supplementary Appendix.

To generate 3D envelopes of motion, we first identified the incisal and condylar points from the f-CBCT model. The *incisal point* was selected as the point on the lower left central incisal edge in the X-Z plane. The *condylar points* were defined as the most superior (distant) point of each condyle based on the length of a perpendicular line from the X-Y plane. For each dataset, we used the first frame of the four cranial sensor locations as a reference and then registered the rest of the frames to the reference points. We determined the start and end of each mandibular trajectory using 3D velocity thresholds, then normalized the trajectory to 100 percent.

Incisal point movements were reconstructed by applying rigid body transformation matrices formed by the microsensors with respect to the four cranial sensors. Condylar movements were reconstructed using the same transformation matrices. No additional filtering was performed for the incisal and condylar movements. Since all movements started from the MIP position, we combined all recorded movements and used the previously identified incisal and condylar points to construct the complete incisal and condylar envelopes of movements.

Tracking performance assessment

To evaluate the tracking performance, we calculated the Euclidean distance between the two microsensors and cranial sensors in the following conditions:

- 1. To represent the overall tracking consistency, we estimated the variability of the Euclidean distance between the two microsensors during all voluntary movements.
- 2. To examine the effect of the metal surgical instruments interference, a metal tongue retractor was moved in and out of the participant's mouth that was held open by a bite block. We calculated the Euclidean distance and ±1 standard deviation (SD) between two microsensors during a "quiet" phase without the tongue retractor. The standard deviation of the distance in the quiet phase was set as threshold for signal distortion. When the tongue retractor was inside the mouth, the Euclidean distance between each microsensor and each of the four cranial sensors was compared against the threshold values during the quiet phase.

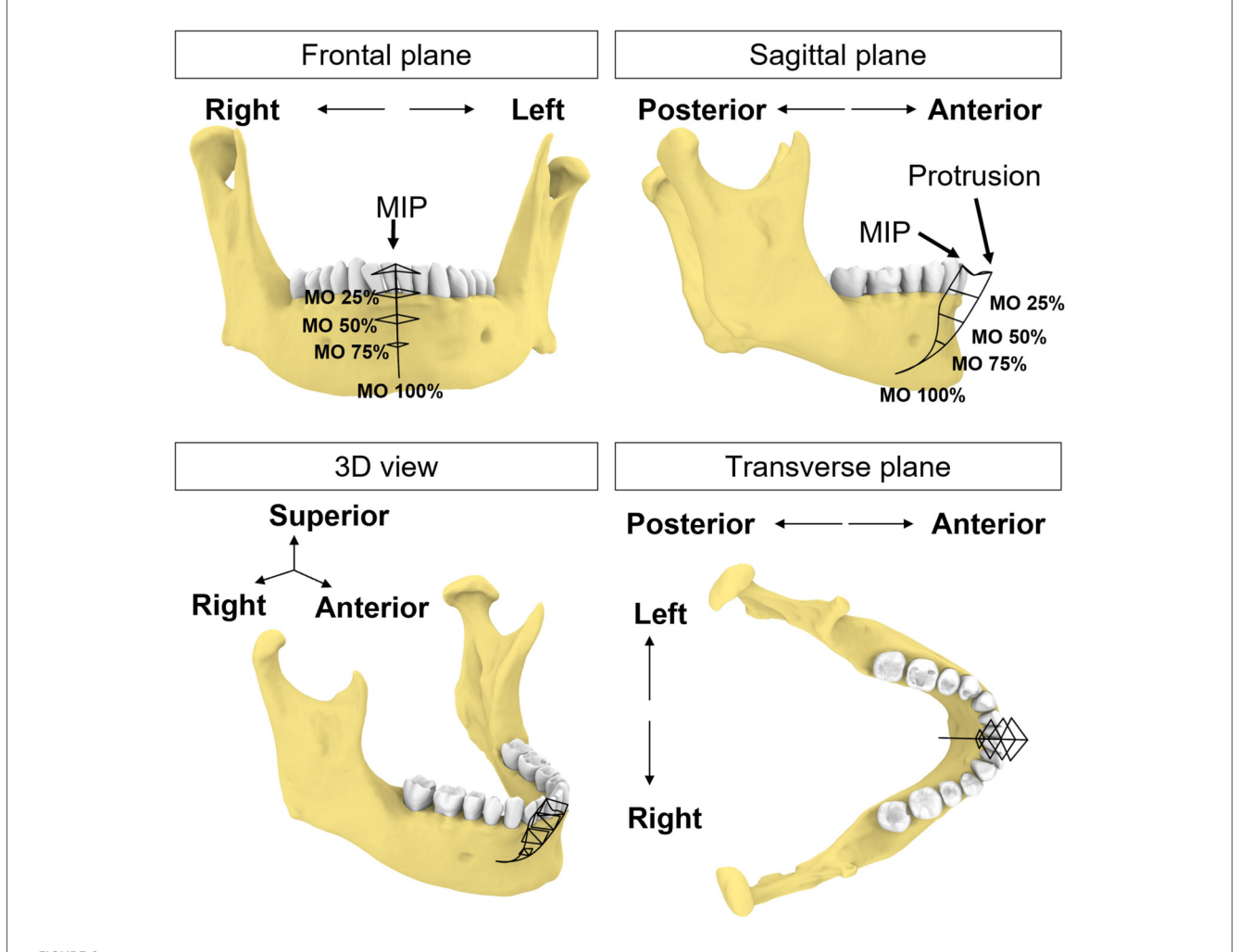


FIGURE 2
Schematic illustration of incisal trajectories (black solid lines). The participant uses this figure as a guide to move the jaw to different levels of mouth opening (MO) starting from MIP position or protruded position.

Simulation

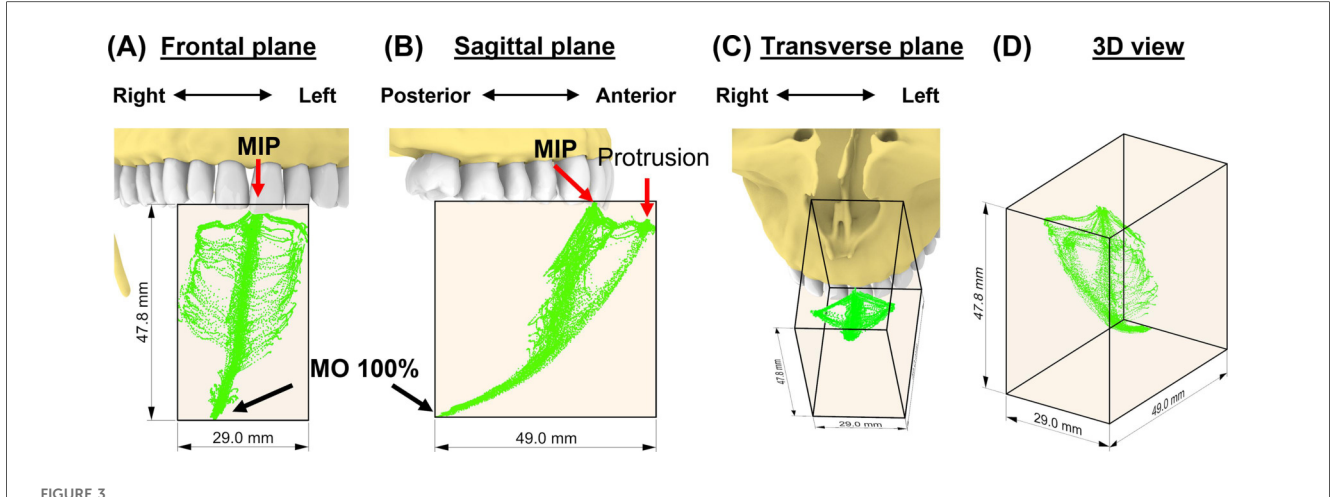
In this section, we simulated four conditions to demonstrate the interplay between the incisal and condylar movements and the importance of simultaneous monitoring of incisal and bilateral condylar points. Simply relying on incisal point alone to represent mandible pose is insufficient and may allow condylar poses outside their envelopes. These simulated cases were selected to portray possible positions during dental procedures. For example, sedated patients have mandible positioned by the clinician conscious patients are instructed to position their mandible, sometimes with assistance by the clinician, to create working space for the dental procedures, such as open their mouth wider or move jaw to left or right. In these simulations, we consider the lower teeth and mandible as a single rigid body based on the assumption that there is no relative movement between any teeth nor between the teeth and the mandible.

Case 1—excessive mouth opening

To replicate a pose that exceeds the subject's maximal mouth opening, we simulated incisal point at 110% of mouth opening. This was calculated based on the incisal trajectories during mouth opening from the most protruded position (0%) to full (100%) mouth opening. For rigid body registration, the mandible was aligned to the simulated incisal point (110% of mouth opening), while keeping the two condylar points at 100% to avoid assumptions on their positions at 110% of mouth opening.

Case 2 – mouth opening with condyles remaining in the fossa

During the early phase of mouth opening, the mandibular condyles remain within the mandibular fossa until the separation between the mandible and the anterior teeth reaches



The subject-specific incisal envelope of movements is shown in the frontal plane (A), sagittal plane (B), transverse plane (C), and in 3D (D) relative to the incisors. A bounding box for the incisal envelope was created to measure the dimensions of the envelope.

20–25 mm. Beyond this point, the mandible begins to translate out of the fossa (38). To provide adequate access for instruments and proper visualization of the back teeth procedures, clinicians would typically need to open the mouth of the patient (under sedation or general anesthesia) to about 40 mm while ensuring the condyles remain in the fossa by not allowing anterior translation (41). Based on these data, we simulated a pose where the condylar points were only rotated along its axis, without translation, until the mouth reached a 40 mm linear distance from the incisal point at MIP.

Case 3—excessive lateral excursion of the jaw

In this simulation, we replicated a pose to expose the upper right molars by shifting an incisor 3 mm beyond the rightmost border of the motion envelope at 50% mouth opening. The condylar points were aligned to the simulated incisal point.

Case 4—lateral excursion of the jaw with greater interocclusal space on the same side as the excursion

This simulation created additional vertical space for the right molar by lateral excursion of the jaw to the right. With the incisal point at 50% mouth opening and at the rightmost position of the envelope, we simulated a 5° rotation along the axis formed by the incisal and left condylar point to increase vertical space for the right molar.

Results

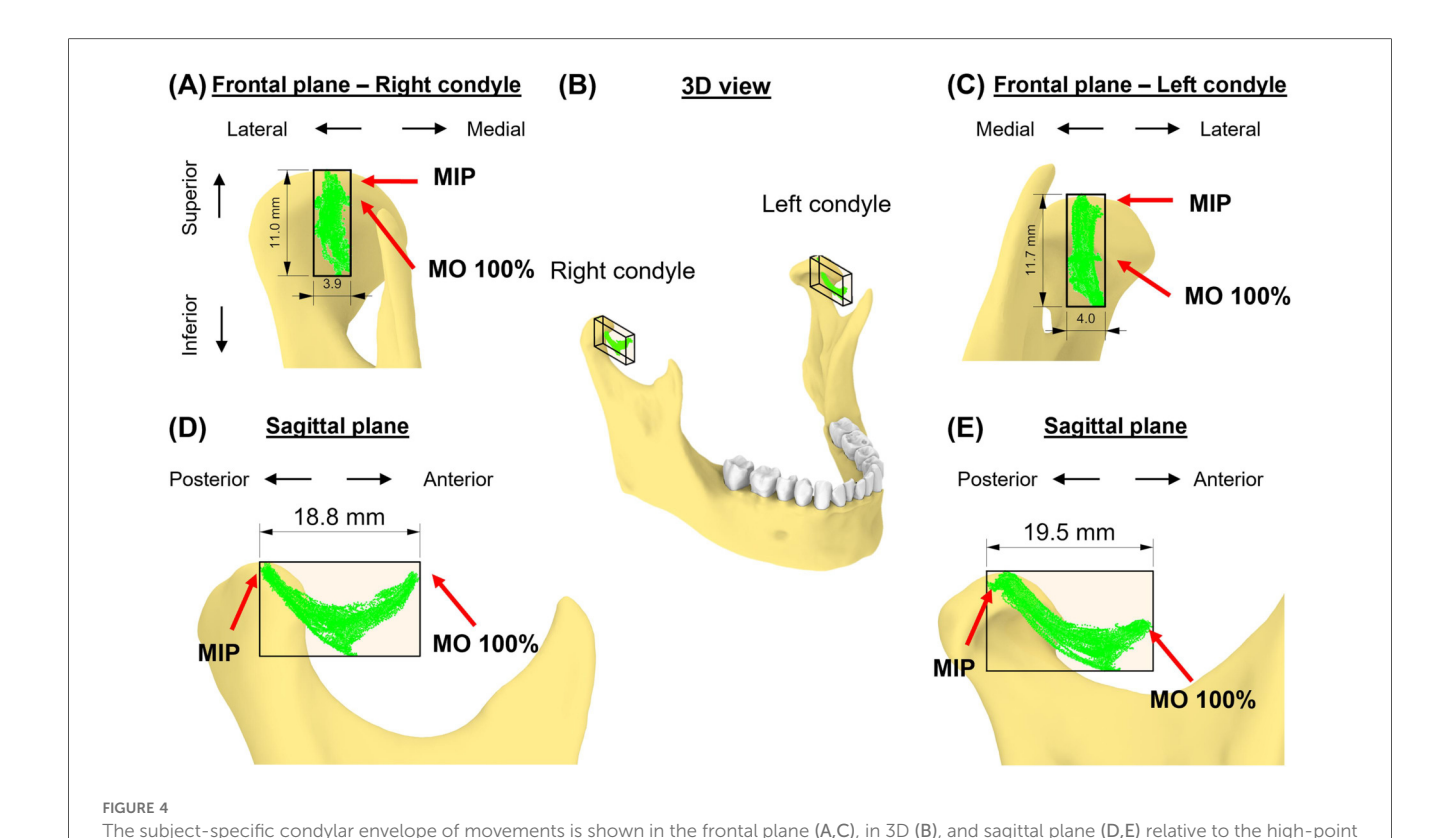
A total of 35 distinct movement tasks were performed, and 175 trials of these movements were analyzed to create the incisal and condylar envelopes of movement.

Incisal envelope of movements

The incisal envelope of movements is characterized by a feather-like shape when trajectories of all instructed mandibular movements were plotted together (Figure 3). As can be viewed from the frontal and transverse planes (Figures 3A-C), this subject made fewer lateral movements to the right. By creating a bounding box (42), we measured the dimensions of the envelope of motion for this subject as 29.0 mm, 47.8 mm, and 49.0 mm along the medial-lateral (ML), anterior-posterior (AP), and superior-inferior (SI) direction, respectively (Figure 3D). Comparison of these dimensions revealed that this participant exhibited an asymmetric incisal envelope that slightly deviated to the right during mouth opening; at full mouth opening, the incisal point is approximately 6.3 mm to the right from the MIP [see frontal plane, (Figure 3A)]. Moreover, the envelope became very narrow at nearly two-thirds of the mouth opening path (Figure 3B).

Condylar envelopes

The 35 movement tasks formed distinct shapes of envelopes for each condyle in the sagittal plane for this subject, whereas the two envelopes were similar in the frontal plane (Figures 4A–C). Specifically, the left condylar envelope was a J-shape while the right was a U-shape (Figures 4D,E). Both right and left condylar points moved inferiorly and anteriorly in the first half of the condylar



of the condyle. A bounding box for the condylar envelope was created to measure the dimensions of the envelope.

path during mouth opening. The right condylar point moved anteriorly and upwardly in the second half (~50% of mouth opening); the left condylar point moved anteriorly. At full mouth opening, the right condylar point was 9 mm upwards compared to the left side of 5 mm. These observations indicate asymmetrical movements between the condyles. Dimension-wise, the differences between the two condylar envelopes were within 1 mm (Table 1).

Consistency assessment

Over the 35 voluntary movement tasks [average recording duration: 28.9 (SD: 6.8) seconds], the standard deviation of the distances between the two microsensors was 0.148 (SD: 0.062) mm (range: 0.040–0.292). In the surgical instrument metal artifact test, a threshold of 0.042 mm distance between positions recorded by microsensors to determine periods of signal distortion (Figure 5A). There were three outcomes: 1. both microsensors were not affected, i.e., the distance between each microsensor and cranial sensors remained within the defined threshold, 2. one of the microsensors had distorted signal, and 3. both microsensors were affected (Figure 5B).

Simulations

In the first simulation (Figure 6), we assessed the effects of an additional 10% mouth opening beyond the subject's maximal

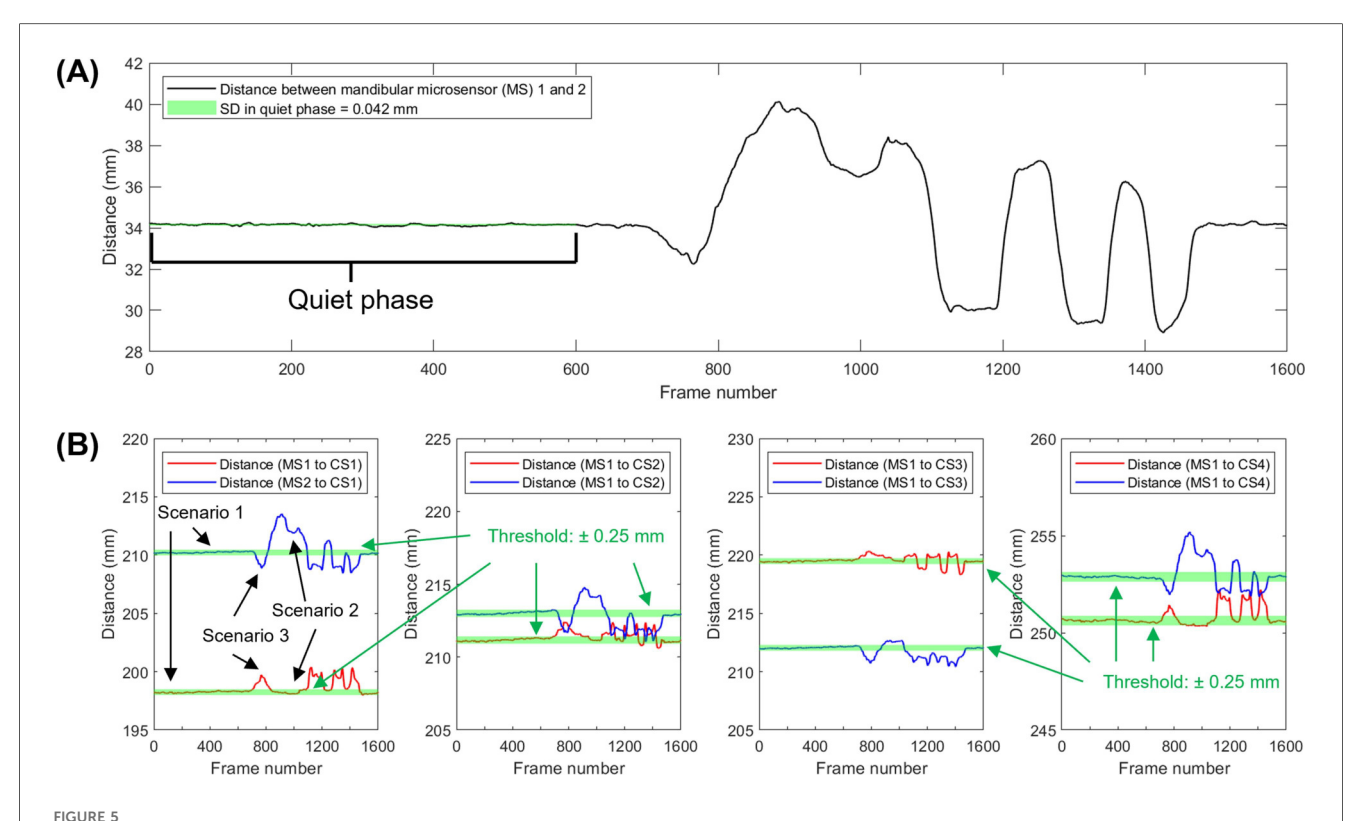
TABLE 1 Dimensions of the condylar envelopes of movements.

Dimension	Left condyle	Right condyle
Medial-lateral (mm)	4.0	3.9
Anterior-posterior (mm)	19.5	18.8
Superior-inferior (mm)	11.7	11.0

voluntary opening. At the maximal protruded position, the mandible rotated 48.4° at 100% mouth opening along a circular path and 53.2° at 110%. At this simulated pose, both left and right condyles were 0.2 and 0.8 mm outside their condylar envelopes (Figures 6A–C). The simulated incisal point was also 6.8 mm outside the incisal envelope (Figures 6D,E). Thus, at 110% mouth opening, the incisal point exhibited the largest deviation from its envelope of motion.

In the second case, we simulated a pose corresponding to a mouth opening of 40 mm (Euclidean distance) from the incisal point at MIP (Figure 7). Mandibular rotation at this simulated pose was 24.1°, placing the incisal point 9.7 mm outside its envelope of motion.

Next, we simulated a jaw position that was shifted laterally (Figure 8). At 50% mouth opening, we shifted the incisal point 3 mm from the rightmost border of the incisal envelope. In this simulated pose, the left condylar point was 2.1 mm outside the envelope while the right condylar point was outside its envelope by 0.1 mm (Figures 8A–C). This indicates that excessive lateral movements (Figures 8D,E) may lead to significant deviations from condylar envelopes, particularly affecting the contralateral condyle.



Approach used to identify sensor signal distortion. (A) Distance between mandibular sensors over time while a metal tongue retractor was placed and removed. (B) Distance between a specific cranial sensor (CS) and the left and right mandibular microsensors (MS). Scenario 1 shows a period of reliable signal from frames from 1–600, around frames 900–1,500, deflections occur which indicate the presence of artifacts. Portions of the data show distortion of only one microsensor (scenario 2) or both microsensors (scenario 3).

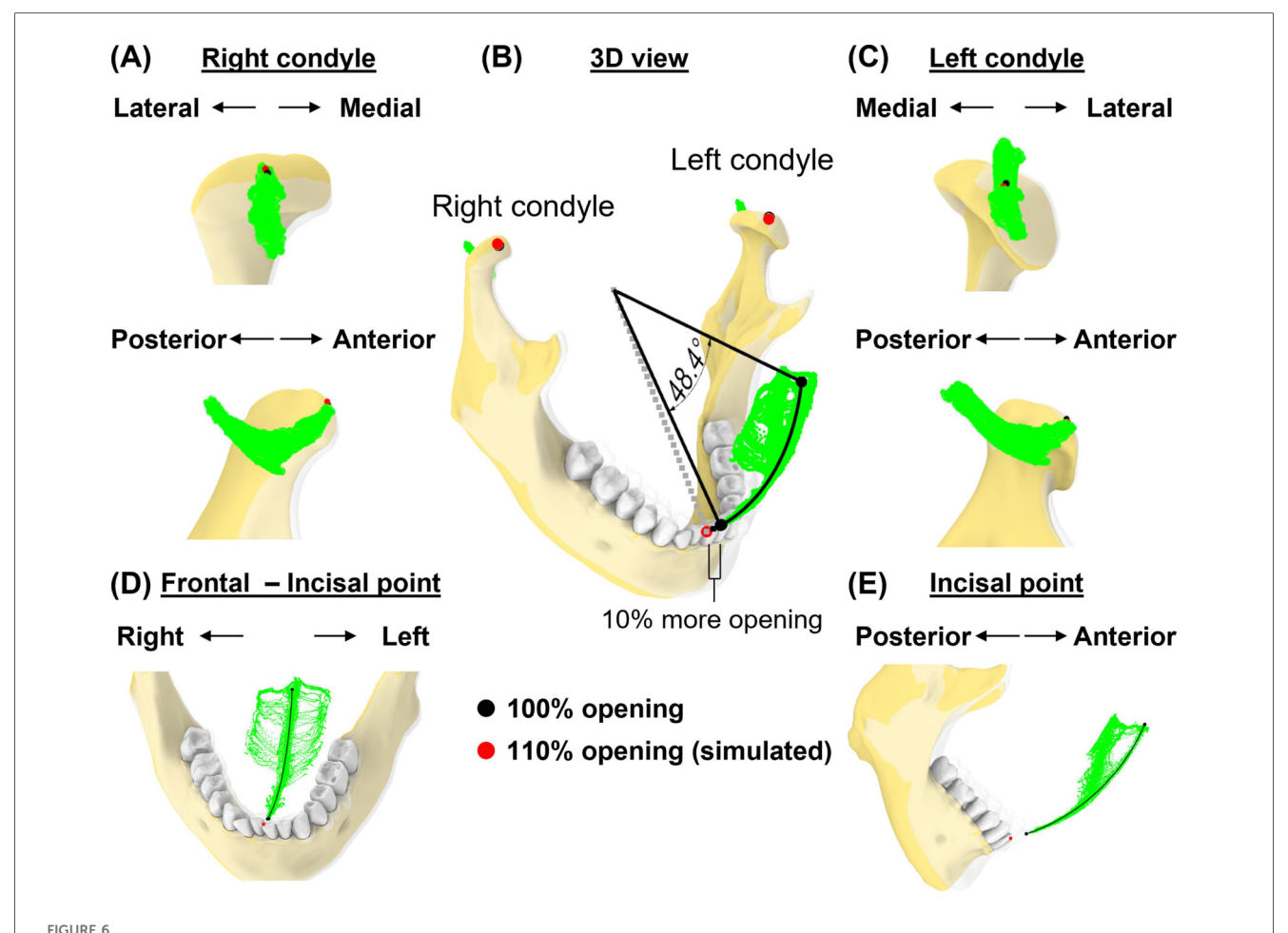
Lastly, we simulated a vertical space creation for posterior tooth procedures. The 5° rotation around the axis connecting the incisor and left condyle (Figures 9A,B) resulted in 7.4 mm linear displacement from the original pose at the right condylar point (Figure 9C). This places the right condyle outside of its envelope. Additionally, the linear distance between the upper and lower 2nd molars increased by 13.0% (from 21.6 mm–24.4 mm, Figure 9D).

Discussion

In this study, we introduced a novel approach for quantifying subject-specific mandibular movement dynamics. By simultaneously monitoring incisal and bilateral condylar envelopes of motion, our approach overcomes the inherent limitations of tracking incisal envelope alone, providing a more comprehensive and accurate 3D representation of mandibular dynamics compared to methods that rely solely on either incisal or condylar path analysis.

Several established methods have been developed to understand the basic functions of mandibular movements. For example, cine CT and cine MRI offers direct visualization of TMJ structures dynamically (29, 43). However, these measurements are not always feasible due to space limitations

and practical challenges during dental procedures. Optical marker tracking system can adequately track voluntary mandibular movements by using external markers extended from the lower teeth (24, 44-45). Optical marker tracking provides good tracking accuracy (46), but relies on a clear line of sight. Therefore, any obstruction can cause tracking loss or errors, necessitating specific clearance for marker visibility during dental procedures. In contrast, the electromagnetic tracking system used in our study eliminates the need for this clearance while providing accuracy comparable to the optical tracking system. However, the electromagnetic tracking system is susceptible to data distortion from metallic artifacts, such as when using metallic tools in the region between the sensor and magnetic source. This can be circumvented by using two microsensors to allow for data recovery in case of missing or distorted data from one of the microsensors. While both microsensors could be affected at the same time, we have presented a postprocessing method to distinguish and remove the distorted data. These results support the potential applicability of this electromagnetic tracking device for accurately tracking jaw movements during clinical procedures, allowing real-time feedback to clinicians. The system used in this study supports third-party plug-ins to stream signals, so the developer can design feedback deliveries, such as haptic, auditory, or visual systems. This is particularly significant in



Simulation case 1. (A) Right condylar points at maximum opening (black) and simulated pose (red) are shown relative to condylar envelope. (B) Incisal and condylar points relative to their envelopes, shown at full mouth opening (transparent jaw) vs. 110% of mouth opening along a circular path. (C), As in (A), but shown for left condyle. (D,E) Frontal and sagittal views show incisal points relative to its envelope.

prolonged dental procedures, such as root canal therapy or the extraction of difficult-to-access impacted third molars on a sedated patient, which are linked to increased TMD prevalence or pain (47–49).

Our novel approach allows for the comparison of subject-specific incisal and condylar envelopes before and after clinical procedures. Combined with spatial and temporal information on mandibular positions during procedures, this information could provide new insights into TMD risk factors. Goldman (8) describes discal attachment injury as occurring when the mandible's range of movement is exceeded or violated and results in tearing or loosening of the lateral discal and/or capsular ligaments. These discal ligaments are well vascularized and innervated and can become inflamed and painful (8) and what began with inflammation can lead to capsulitis. Injuries could occur, if a sedated patient's mandible is moved passively near or beyond its borders, defined by awakened voluntary movements, that leads to ligaments and soft tissues being stretched or injured in positions that relate to rotational and translational movements of the

mandible that are not obvious by examining a single incisal or condylar point relative to it its typical range of motion envelope.

The incisal envelope of movements generated in this study extends past research, which largely concentrated on sagittal plane movements, such as mouth opening and closing, or frontal plane side-to-side excursions. Past research which concentrated on sagittal plane movements has shown that incisal linear distance could be under 40 mm for patients with degenerative TMJ disorder (33), an average of low to mid-50 mm for adults (50, 51), and as high as 65.5 mm for orthodontic patients with different skeletal patterns (21). Importantly, about half of the sample in the studies have a mean maximal opening smaller than the average value. The transverse plane at different levels of opening and combinedplane movements have not been studied explicitly (44). The movement tasks outlined in this study could enable a more thorough construction of the "envelope of motion," capturing both incisal and condylar movements completely. Recently, our group has validated the use of a self-instructional video to create

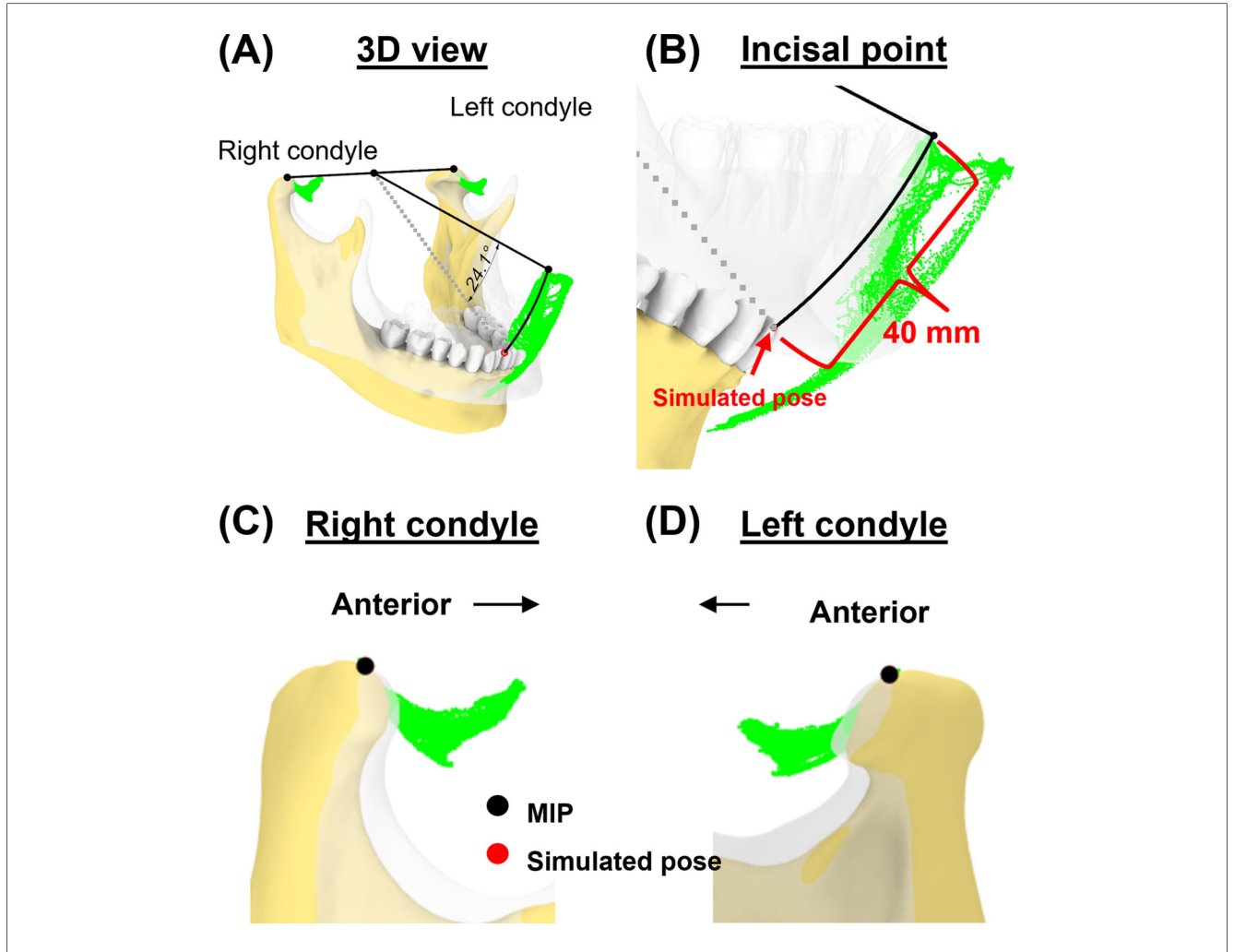


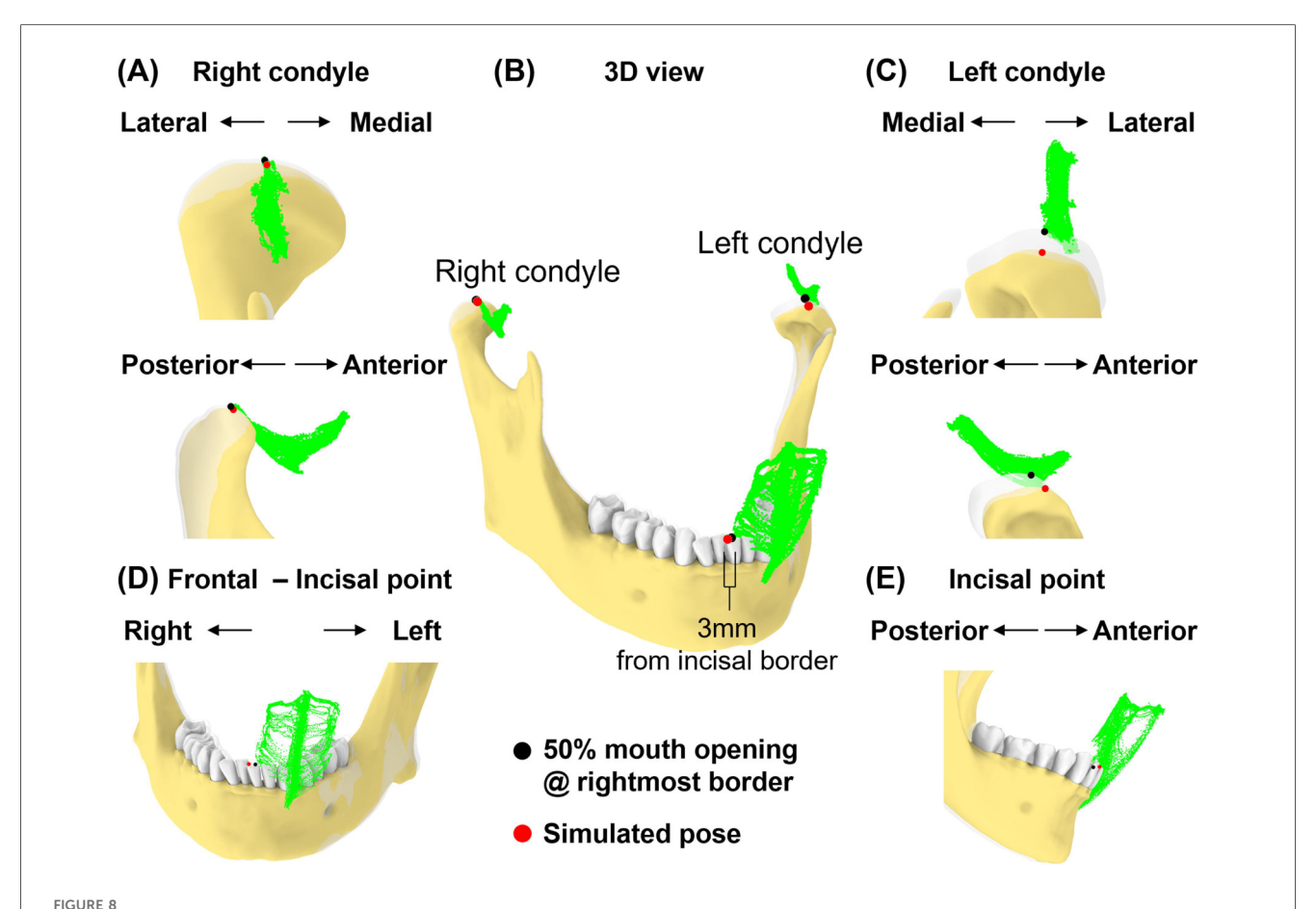
FIGURE 7
Simulation case 2. (A) Two condylar points were used to create a rotational axis for simulating a 40-mm mouth opening. (B) Simulated incisal point is shown outside the incisal envelope of movement. (C,D) Condylar points at simulated pose remain unchanged.

a standard 3D envelope in 10 subjects aged 19–22 (52). While an instructional video might help in reducing intra-subject variability, we recommend using the most extreme values that a subject produces voluntarily from multiple trials to create the "maximal comfortable 3D envelope of motion" for each subject. Not using the average across trials aligns with the common practice that clinicians record maximal incisal opening performed voluntarily and then measure the "assisted" maximal opening when the clinician manually opens the jaw further. Our hypothesis is that the degree of violating the "maximal comfortable 3D envelope of motion" in specific 3D locations may be related to subsequent pain complaints.

There is a shape difference but slight variation in terms of dimensions between the two condylar envelopes of movement in our case study. The AP dimension in both condyles is less than 20 mm, which is consistent with the values reported in earlier research. Baltali and colleagues (33) reported AP condylar path of approximately 2 cm during mouth opening

and closing for patients with degenerative TMJ disorder. Salaorni and Palla (51) reported slightly smaller condylar translations during mouth opening and closing (14 ± 4.2 mm). Yatabe and colleagues (53, 54) used OKAS-3D recording system, which does not include subject-specific imaging-based geometry, and reported the length of condylar movements in protrusive-retrusive movement and mouth opening-closing for approximately 23 mm for both condyles (SD: \sim 4 mm). Huang and colleagues (44) reported approximately 19 mm (SD: 4 mm) mouth opening and smaller movements during protrusion. Our study also demonstrates the presence of medio-lateral movements in the TMJ, although the range in this dimension is smaller compared to other dimensions, such as AP and SI movements. This finding is consistent with a study using single fluoroscopic imaging (28).

The incorporation of incisal and condylar tracking extends beyond jaw movement monitoring. The generated data allows for simulations that are useful for dental clinical practice, such as surgical planning and evaluation of potential risks of



Simulation case 3. (A) Right condyle positions at 50% mouth opening to the rightmost border and simulated pose are shown relative to condylar envelope. (B) Illustration of a 3 mm incisal displacement to the right of the border of incisal envelope. Incisal and condylar points relative to their envelopes, shown at 50% opening with displacement to the rightmost border (transparent jaw) and simulated pose. (C) As in (A), but shown for left condyle. (D,E) Frontal and sagittal views show incisal point at 50% opening with displacement to the rightmost of the border and simulated pose relative to its envelope.

procedures to patients, and even as an aid for physical therapy of TMJ pain or dysfunctions. Our simulated cases demonstrated that excessive mouth opening, or lateral excursion could result in asymmetric condylar displacement. This implies that conditions that cause excessive jaw translation and rotation may result in traumatic injuries to tissues around the condyles, such as the discal and sphenomandibular ligaments. Similarly, the elongation pattern of sphenomandibular or stylomandibular ligaments can be simulated to predict the impact of certain intraoral procedures. Understanding the interaction between ligament status and duration of loading can further enhance our knowledge of TMJ function and its implications for dental care.

This study reports data from a single participant with different simulated poses and is therefore not generalizable to larger populations across age, sex, or multiple collection sites. The primary goal of this study was not to provide population-level estimates but to describe and demonstrate a novel method for quantifying mandibular motion, using actual data from one subject alongside simulated poses. While simulated poses are commonly used to explain clinical cases, future studies are

needed to document and quantify actual occurrences of motion beyond the voluntary comfortable 3D envelope in clinical populations, ideally across larger samples stratified by demographic factors. Planned future work includes validating whether the simulated poses in patients under deep sedation occur during third molar removal by capturing real movements that exceed the voluntary range. In addition, although microsensors were securely affixed with light-cure adhesive and inspected for integrity before data collection, potential displacement is conceptually possible (e.g., debonding between the microsensor within the retainer). As described in the "tracking consistency" section, between-sensor displacement can be detected, and in the event of one sensor on the lower retainer displacement, the unaffected sensor could still provide usable data. The displacement of the retainer, affecting both microsensors, is possible, but can be detected through observation by clinicians and researchers and self-reporting by participants. Nonetheless, such scenarios were not observed in the present study, and further testing under varied clinical conditions will be necessary to fully evaluate system robustness.

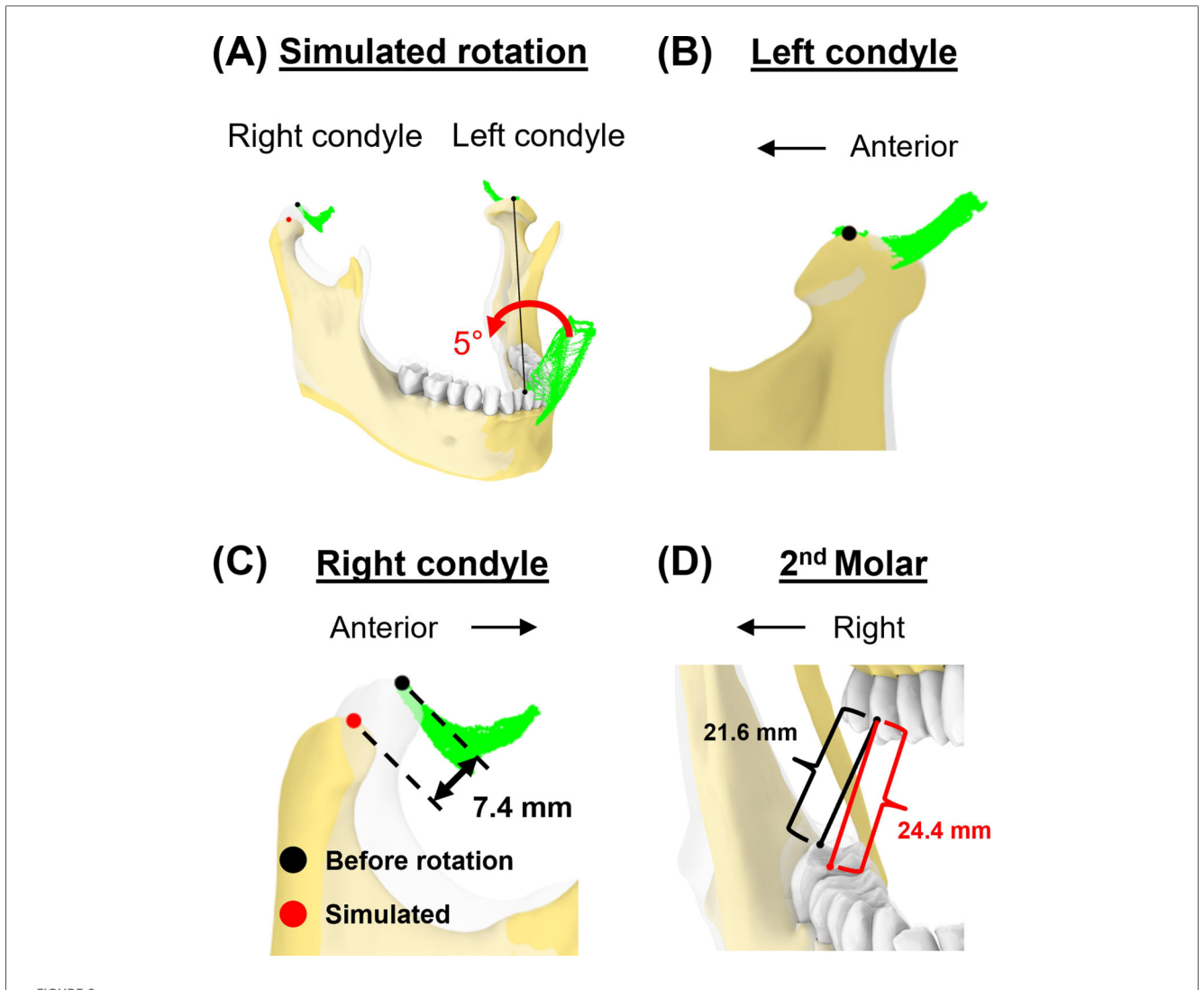


FIGURE 9 Simulation case 4. (A) The mandible is rotated for 5° around the axis connecting incisor and left condyle. (B) Left condylar point remains unchanged. (C) In this simulated pose, the right condyle was displaced by 7.4 mm. (D) The distance between the upper and lower second molars increased.

Conclusion

Our novel approach to quantifying subject-specific, dynamic incisal and condylar movements represents a significant advancement in TMJ biomechanics. By simultaneously tracking both incisal and condylar motion envelopes, we provide novel insight into the complex threedimensional kinematics of mandibular function. This integrated perspective reveals critical relationships that remain invisible to traditional single-landmark tracking methods. While our findings demonstrate potential for clinical application, further validation across diverse patient populations is essential to refine this methodology and establish normative parameters. The next critical phase of research must focus on correlating these biomechanical measurements with clinical outcomes and patient-reported symptoms. By integrating our understanding of TMJ kinematics into clinical practice, we can potentially prevent damage to TMJ structures, develop targeted interventions for TMD, establish evidence-based parameters for safe mandibular manipulation during dental procedures, and improve individual patient outcomes.

Data availability statement

The raw data supporting the conclusions of this article will be made available by the authors, without undue reservation.

Ethics statement

The requirement of ethical approval was waived by Institutional Review Board at the University of Washington for the studies involving humans because The IRB determined that measuring how one of the authors own lower jaw moves

through space doesn't meet the regulatory definition of research. In other words, we would not consider collecting data about just one of the authors to be a *systematic* investigation that is designed to develop or contribute to generalizable knowledge. This means that this activity does not require IRB review. The studies were conducted in accordance with the local legislation and institutional requirements. The ethics committee/institutional review board also waived the requirement of written informed consent for participation from the participants or the participants' legal guardians/next of kin because The sole human participant is one of the authors.

Author contributions

JL: Conceptualization, Formal analysis, Investigation, Methodology, Software, Visualization, Writing - original draft, Writing - review & editing. DR: Conceptualization, Formal analysis, Funding acquisition, Investigation, Methodology, Project administration, Resources, Writing review & editing. AB: Conceptualization, Funding acquisition, Investigation, Supervision, Writing - review & editing. GH: Funding acquisition, Investigation, Project administration, Writing - review & editing. FA-M: Conceptualization, Formal analysis, Funding acquisition, Investigation, Methodology, Project administration, Supervision, Writing - review & editing.

Funding

The author(s) declare that no financial support was received for the research and/or publication of this article.

Acknowledgments

The authors thank Dr. Roozbeh Khosravi for his technical assistance.

References

- 1. National Institute of Dental and Craniofacial Research. Prevalence of TMJD and its Signs and Symptoms (2018). Available online at: https://www.nidcr.nih.gov/research/data-statistics/facial-pain/prevalence (Accessed August 20, 2024).
- 2. National Academies of Sciences E and M. Temporomandibular disorders: priorities for research and care. In: Bond EC, Mackey S, English R, Liverman CT, Yost O, editors. *Temporomandibular Disorders: Priorities for Research and Care.* Washington, DC: The National Academies Press (2020). p. 1–3. Available online at: https://nap.nationalacademies.org/catalog/25652/temporomandibular-disorders-priorities-for-research-and-care (Accessed August 20, 2024).
- 3. Kapos FP, Exposto FG, Oyarzo JF, Durham J. Temporomandibular disorders: a review of current concepts in aetiology, diagnosis and management. *Oral Surg.* (2020) 13(4):321–34. doi: 10.1111/ors.12473
- 4. Huang GJ, LeResche L, Critchlow CW, Martin MD, Drangsholt MT. Risk factors for diagnostic subgroups of painful temporomandibular disorders (TMD). *J Dent Res.* (2002) 81(4):284–8. doi: 10.1177/154405910208100412

Conflict of interest

The authors declare that the research was conducted in the absence of any commercial or financial relationships that could be construed as a potential conflict of interest.

Generative AI statement

The author(s) declare that Generative AI was used in the creation of this manuscript. The author(s) verify and take full responsibility for the use of generative AI in the preparation of this manuscript. Generative AI was used for grammar checking in this manuscript.

Any alternative text (alt text) provided alongside figures in this article has been generated by Frontiers with the support of artificial intelligence and reasonable efforts have been made to ensure accuracy, including review by the authors wherever possible. If you identify any issues, please contact us.

Publisher's note

All claims expressed in this article are solely those of the authors and do not necessarily represent those of their affiliated organizations, or those of the publisher, the editors and the reviewers. Any product that may be evaluated in this article, or claim that may be made by its manufacturer, is not guaranteed or endorsed by the publisher.

Supplementary material

The Supplementary Material for this article can be found online at: https://www.frontiersin.org/articles/10.3389/fdmed. 2025.1654118/full#supplementary-material

- 5. Sharma S, Wactawski-Wende J, Lamonte MJ, Zhao J, Slade GD, Bair E, et al. Incident injury is strongly associated with subsequent incident temporomandibular disorder: results from the OPPERA study. *Pain*. (2019) 160(7):1551–61. doi: 10.1097/j.pain.000000000001554
- 6. Sharma S, Ohrbach R, Fillingim RB, Greenspan JD, Slade G. Pain sensitivity modifies risk of injury-related temporomandibular disorder. *J Dent Res.* (2020) 99(5):530–6. doi: 10.1177/0022034520913247
- 7. Ohrbach R, Sharma S. Temporomandibular disorders: definition and etiology. Semin Orthod. (2024) 30(3):237–42. doi: 10.1053/j.sodo.2023.12.011
- 8. Goldman JR. Soft tissue trauma. In: Kaplan AS, Assael LA, editors. Temporomandibular Disorders: Diagnosis and Treatment. Philadelphia: W.B. Saunders (1991). p. 190–223.
- 9. Damasceno YSS, Espinosa DG, Normando D. Is the extraction of third molars a risk factor for the temporomandibular disorders? A systematic review. *Clin Oral Investig.* (2020) 24(10):3325–34. doi: 10.1007/s00784-020-03277-6

- 10. Huang GJ, Rue TC. Third-molar extraction as a risk factor for temporomandibular disorder. *J Am Dent Assoc.* (2006) 137(11):1547–54. doi: 10. 14219/jada.archive.2006.0090
- 11. Woodford SC, Robinson DL, Mehl A, Lee PVS, Ackland DC. Measurement of normal and pathological mandibular and temporomandibular joint kinematics: a systematic review. *J Biomech.* (2020) 111:109994. doi: 10.1016/j.jbiomech.2020.109994
- 12. Pertes RA, Gross SG. Clinical Management of Temporomandibular Disorders and Orofacial Pain. Temporomandibular Disorders and Orofacial Pain. Chicago: Quintessence Pub. (1995).
- 13. Iturriaga V, Bornhardt T, Velasquez N. Temporomandibular joint: review of anatomy and clinical implications. *Dent Clin North Am.* (2023) 67(2):199–209. doi: 10.1016/j.cden.2022.11.003
- 14. Wilkie G, Al-Ani Z. Temporomandibular joint anatomy, function and clinical relevance. Br Dent J. (2022) 233(7):539–46. doi: 10.1038/s41415-022-5082-0
- 15. Bordoni B, Varacallo M. Anatomy, head and neck, temporomandibular joint. In: *StatPearls*. Treasure Island, FL: StatPearls Publishing (2023). Available online at: https://www.ncbi.nlm.nih.gov/books/NBK538486/ (Accessed October 7, 2024).
- 16. Tanaka E, Van Eijden T. Biomechanical behavior of the temporomandibular joint disc. *Crit Rev Oral Biol Med.* (2003) 14(2):138–50. doi: 10.1177/154411130301400207
- 17. Posselt U. Studies in the mobility of the human mandible. *Acta Odontologica Scandinavica*. (1953) 10(Supplementum 10).
- 18. Posselt U. Movement areas of the mandible. *J Prosthet Dent.* (1957) 7(3):375–85. doi: 10.1016/S0022-3913(57)80083-3
- 19. Posselt U. An analyzer for mandibular positions. *J Prosthet Dent.* (1957) 7(3):368–74. doi: 10.1016/S0022-3913(57)80082-1
- 20. Ueki K, Moroi A, Takayama A, Tsutsui T, Saito Y, Yoshizawa K. Evaluation of border movement of the mandible before and after orthognathic surgery using a kinesiograph. *J Craniomaxillofac Surg.* (2020) 48(5):477–82. doi: 10.1016/j.jcms.2020.02.021
- 21. Farfán NC, Lezcano MF, Navarro-Cáceres PE, Sandoval-Vidal HP, Martinez-Gomis J, Muñoz L, et al. Characterization of mandibular border movements and mastication in each skeletal class using 3D electromagnetic articulography: a preliminary study. *Diagnostics*. (2023) 13:2405. doi: 10.3390/diagnostics13142405
- 22. Laskin DM, Greene CS, Hylander WL. Temporomandibular Disorders: An Evidence-Based Approach to Diagnosis and Treatment. TMDs. Chicago: Quintessence Pub. (2006).
- 23. Ahlers MO, Petersen T, Katzer L, Jakstat HA, Roehl JC, Türp JC. Condylar motion analysis: a controlled, blinded clinical study on the interindividual reproducibility of standardized evaluation of computer-recorded condylar movements. *Sci Rep.* (2023) 13(1):1–14. doi: 10.1038/s41598-023-37139-4
- 24. Shu J, Feng Y, Zheng T, Shao B, Liu Z. Temporomandibular condylar articulation and finite helical axis determination using a motion tracking system. *Med Eng Phys.* (2021) 94:80–6. doi: 10.1016/j.medengphy.2021.06.007
- 25. Kim D, Hwang S, Choi S, Lee S, Heo M, Heo K. Quantitative Analysis of the TMJ Movement with a New Mandibular Movement Tracking and Simulation System (2008). Available online at: https://s-space.snu.ac.kr/handle/10371/73559 (Accessed October 9, 2024).
- 26. Visscher CM, Huddleston Slater JJR, Lobbezoo F, Naeije M. Kinematics of the human mandible for different head postures. J Oral Rehabil. (2000) 27(4):299–305. doi: 10.1046/j.1365-2842.2000.00518.x
- 27. Baltali E, Zhao KD, Koff MF, Keller EE, An KN. Accuracy and precision of a method to study kinematics of the temporomandibular joint: combination of motion data and CT imaging. *J Biomech.* (2008) 41(11):2581–4. doi: 10.1016/j. ibiomech.2008.05.023
- 28. Chen CC, Lin CC, Lu TW, Chiang H, Chen YJ. Feasibility of differential quantification of 3D temporomandibular kinematics during various oral activities using a cone-beam computed tomography-based 3D fluoroscopic method. *J Dent Sci.* (2013) 8(2):151–9. doi: 10.1016/j.jds.2012.09.025
- 29. Helms CA, Gillespy T, Gould RG, Ware WH. Cine-CT of the temporomandibular joint. *Cranio*. (1986) 4(3):246–50. doi: 10.1080/08869634.1986.11678151
- 30. Travers KH, Buschang PH, Hayasaki H, Throckmorton GS. Associations between incisor and mandibular condylar movements during maximum mouth opening in humans. *Arch Oral Biol.* (2000) 45(4):267–75. doi: 10.1016/S0003-9969(99)00140-5
- 31. Shu J, Ma H, Liu Y, Zheng T, Shao B, Liu Z. *In vivo* biomechanical effects of maximal mouth opening on the temporomandibular joints and their relationship to morphology and kinematics. *J Biomech.* (2022) 141:111175. doi: 10.1016/j. ibiomech.2022.111175
- 32. Koolstra JH, Naeije M, Van Eijden TMGJ. The three-dimensional active envelope of jaw border movement and its determinants. J Dent Res. (2001) 80(10):1908–12. doi: 10.1177/00220345010800100901

- 33. Baltali E, Zhao KD, Koff MF, Durmuş E, An KN, Keller EE. A method for quantifying condylar motion in patients with osteoarthritis using an electromagnetic tracking device and computed tomography imaging. *J Oral Maxillofac Surg.* (2008) 66(5):848–57. doi: 10.1016/j.joms.2008.01.021
- 34. Shu J, Ma H, Xiong X, Shao B, Zheng T, Liu Y, et al. Mathematical analysis of the condylar trajectories in asymptomatic subjects during mandibular motions. *Med Biol Eng Comput.* (2021) 59(4):901–11. doi: 10.1007/s11517-021-02346-6
- 35. Xu B, Park JJ, Kim SH. Correlations of temporomandibular joint morphology and position using cone-beam computed tomography and dynamic functional analysis in orthodontic patients: a cross-sectional study. *Korean J Orthod.* (2024) 54(5):325–41. doi: 10.4041/kjod24.089
- 36. Baldini B, Papasratorn D, Fagundes FB, Fontenele RC, Jacobs R. Validation of a novel tool for automated tooth modelling by fusion of CBCT-derived roots with the respective IOS-derived crowns. *J Dent.* (2025) 153:105546. doi: 10.1016/j.jdent.2024. 105546
- 37. Besl PJ, McKay ND. A method for registration of 3-D shapes. IEEE Trans Pattern Anal Mach Intell. (1992) 14(2):239–56. doi: 10.1109/34.121791
- 38. Okeson JP. Management of Temporomandibular Disorders and Occlusion. 6th ed. St. Louis, MO: Mosby Elsevier (2007).
- 39. Polhemus. Polhemus VIPER System Product Specifications. Available online at: https://polhemus.com/_assets/img/Viper_Brochure_1.pdf (Accessed April 14, 2025).
- 40. Ashmore JL, Kurland BF, King GJ, Wheeler TT, Ghafari J, Ramsay DS. A 3-dimensional analysis of molar movement during headgear treatment. *Am J Orthod Dentofacial Orthop.* (2002) 121(1):18–29. doi: 10.1067/mod.2002.120687
- 41. McCain JP, Montero J, Ahn DY, Hakim MA. Arthroscopy and arthrocentesis of the temporomandibular joint. In: Miloro M, Ghali GE, Larsen PE, Waite P, editors. Peterson's Principles of Oral and Maxillofacial Surgery. Cham: Springer. (2022). p. 1569–624. doi: 10.1007/978-3-030-91920-7 53
- 42. Suzuki A. A study on mandibular movement in six degree-of-freedom with a newly developed jaw movement analyzer. *Nihon Hotetsu Shika Gakkai Zasshi.* (1987) 31(3):712–25. doi: 10.2186/jjps.31.712
- 43. Chen J, Buckwalter K. Displacement analysis of the temporomandibular condyle from magnetic resonance images. *J Biomech.* (1993) 26(12):1455–62. doi: 10.1016/0021-9290(93)90096-W
- 44. Huang C, Xu X, Li L, Sun Y, Guo C. Study on the reconstruction of a four-dimensional movement model and the envelope surface of the condyle in normal adults. *Br J Oral Maxillofac Surg.* (2022) 60(7):884–9. doi: 10.1016/j.bjoms.2021.08.
- 45. da Cunha DV, Degan VV, Vedovello Filho M, Bellomo DP, Silva MR, Furtado DA, et al. Real-time three-dimensional jaw tracking in temporomandibular disorders. *J Oral Rehabil.* (2017) 44(8):580–8. doi: 10.1111/joor.12521
- 46. Topley M, Richards JG. A comparison of currently available optoelectronic motion capture systems. J Biomech. (2020) 106:109820. doi: 10.1016/j.jbiomech. 2020.109820
- 47. Dolatabadi MA, Lassemi E. Trauma to the temporomandibular joint following tooth extraction via dental students. *Trauma Mon.* (2012) 16(4):205. doi: 10.5812/traumamon.3432
- 48. Sahebi S, Moazami F, Afsa M, Nabavi Zade MR. Effect of lengthy root canal therapy sessions on temporomandibular joint and masticatory muscles. *J Dent Res Dent Clin Dent Prospects*. (2010) 4(3):95–7. doi: 10.5681/joddd.2010.024
- 49. Hawkins J, Durham P. Prolonged jaw opening promotes nociception and enhanced cytokine expression. J Oral Facial Pain Headache. (2016) 30(1):34-41. doi: 10.11607/ofph.1557
- 50. Khare N, Patil SB, Kale SM, Sumeet J, Sonali I, Sumeet B. Normal mouth opening in an adult Indian population. *J Maxillofac Oral Surg.* (2012) 11(3):309–13. doi: 10.1007/s12663-012-0334-1
- $51.\,Salaorni$ C, Palla S. Condylar rotation and anterior translation in healthy human temporomandibular joints. Schweiz Monatsschr Zahnmed. (1994) 104(4):415–22.
- 52. Cheng YC, Huang GJ, Li JS, Arce-McShane FI, Ramsay DS. A self-instructional training video to perform 3D mandibular border movements. *J Dent Res.* (2025) 104 (B):3278. Available online at: https://iadr.abstractarchives.com/abstract/25iags-427553/a-self-instructional-training-video-to-perform-3d-mandibular-border-provements.
- 53. Yatabe M, Zwijnenburg A, Megens CCEJ, Naeije M. The kinematic center: a reference for condylar movements. *J Dent Res.* (1995) 74(10):1644–8. doi: 10.1177/00220345950740100401
- 54. Yatabe M, Zwijnenburg A, Megens CCEJ, Naeije M. Movements of the mandibular condyle kinematic center during jaw opening and closing. *J Dent Res.* (1997) 76(2):714–9. doi: 10.1177/00220345970760021301